

Phase diagrams of polyethylene blends by Raman spectroscopy*

Jianguo Wang, Deren Pang, and Baotong Huang**

Changchun Institute of Applied Chemistry, Academia Sinica, Changchun, Jilin 130022,
People's Republic of China

SUMMARY

The Raman internal mode region analysis of polyethylene (PE) is extended to studies of blends of different PEs so as to obtain a phase diagram showing the magnitude of crystalline (P_c), amorphous (P_a) and interfacial (P_b) phases at different compositions. The non-cocrystallizable HDPE/LDPE blends shows additivity in phase structure with blend composition. Enlarged share of P_b is seen for compatible blends of HDPE/LLDPE and especially for HDPE with VLDPE of low crystallinity. This method offers an easy access to direct observing compatibility of different PEs on a molecular level.

INTRODUCTION

The blending of different polyethylenes (PEs) helps to regulate physical properties, such as modulus and toughness, and to improve processing behavior of the material. Compatibility of PEs differing materially in type and degree of branching is characterized by their cocrystallizability. Not to mention the teeming structural studies of individual PEs, blends of PEs have been examined for different structural levels by various experimental methods.

Differential scanning calorimetry (DSC) is widely used in judging compatibility (1-4) through information of transitions (T_m , T_c). Of methods probing morphological and supermolecular structures, wide-angle X-ray diffraction (WAXD) (2-4), small-angle X-ray scattering (SAXS) (2-4), small-angle light scattering (SALS) (2-4) and Raman longitudinal acoustic mode scattering (Raman LAM) (2) are powerful tools. Recently time-resolved SAXS with synchrotron radiation has been applied to a study of PE blends (5). No method applicable to studies of PE blends on molecular levels, however, is found in the literature to our knowledge.

*Supported by Chinese Petrochemical Corporation (SINOPEC)

**To whom correspondence should be addressed

The existence of three states of order in a semi-crystalline PE (crystalline, amorphous and interfacial regions) has been recognized by broad-line ^1H NMR(6) and ^{13}C NMR(7), and Raman spectroscopy(8,9) studies. Flory and Yoon(10,11) discussed in detail the nature of the interfacial transition region in terms of lattice theory, the reiteration of which is beyond the scope of this paper. In this work, we extend the Raman internal mode analysis(12,13) to blends of different PEs so that phase diagrams showing their interfacial interaction on a molecular level can be visualized in ease.

EXPERIMENTAL

Polyethylene samples used in this work are listed in Table 1. The very low density polyethylene (VLDPE) samples were synthesized in this laboratory by slurry copolymerization of ethylene and octene-1 using MgCl_2 -supported Ti catalyst(14). Blends of different PEs of Table 1 were prepared in the ratio of 1:3, 1:1 or 3:1 by pouring their hot, homogeneous 1% toluene solution (0.01% antioxidant 246 added) into ethanol, collected and washed with ethanol, and dried in vacuo at 60°C for 3 days.

Table 1 Samples Used in This Work

PE	Source	MI	Branching ($\text{CH}_3/100\text{C}$)
HDPE	Gaoqiao, Shanghai	2	< 2
LDPE	Daqing	2-3	26
LLDPE	Union Carbide	2.1	22
VLDPE	This Laboratory	1.9	~65

Raman spectroscopy was taken on a Dilor Z-24 Laser Raman Spectrometer in conjunction with an Argon ion laser ($=5145 \text{ \AA}$) and a computer system. The process is similar to that described by Glotin and Mandelkern(9).

Specimens of HDPE/LDPE and HDPE/LLDPE blends for Raman measurements were pressed and slowly cooled (SC) in the hot press. For HDPE/VLDPE blends, in order to observe the effect of thermal history, one series of samples was slowly cooled as above but another quenched in ice-water (QC) after being removed from the hot press.

Analysis of bands in the Raman internal mode regions(8) according to

$$\alpha_c = I_{1415}/I_T \times 0.46, \quad \alpha_a = I_{1303}/I_T, \quad \alpha_b = 1 - \alpha_c - \alpha_a$$

gave the fractions of the crystalline (α_c), amorphous (α_a) and interfacial (α_b) regions. α being replaced by F in this work.

RESULTS AND DISCUSSION

In the assignment of bands in the Raman spectra of semi-crystalline polyethylenes, three internal mode region were recognized⁽⁹⁾: (a) skeletal C-C stretching vibration (1000-1200 cm^{-1}), (b) CH_2 -twisting vibration (near 1300 cm^{-1}) and (c) CH_2 -bending vibration (1400-1500 cm^{-1}). An analysis of these bands led to the calculation of the amounts of crystalline phase and the amorphous phase and the concept of the existence of an interfacial anisotropic disordered region, in which chains are in extended trans configuration without lateral order^(8,9).

Application of Raman internal mode analysis to PE blends has only been casually mentioned without further elaboration (15): a 50/50 HPB (hydrogenated polybutadiene)/linear PE blend showed an increase in P_b (19.5%) over that of the homopolymers (6.5% for linear PE and 13.2 for HPB). In the present work, it is shown that phase diagrams showing the fractions of the three phases—crystalline (P_c), amorphous (P_a) and interfacial (P_b) at different PE blend compositions could be constructed, giving a visual comprehension of the phase distribution. Experimental data in Table 2 are plotted into phase diagrams in Fig. 1-4.

Table 2 Phase Structure of PE Blends as Determined by Raman Spectroscopy

Blends	Composition (wt. ratio)	P_c	P_a	P_b ¹⁾
HDPE/VLDPE (SC)	100/ 0	81	14	5
	75/ 25	66	18	16
	50/ 50	52	24	24
	25/ 75	33	48	19
	0/100	15	71	14
HDPE/VLDPE (QC)	100/ 0	75	14	11
	75/ 25	55	25	20
	50/ 50	34	40	26
	25/ 75	19	59	22
	0/100	7	79	14
HDPE/LDPE (SC)	100/ 0	81	14	5
	75/ 25	68	26	6
	50/ 50	57	34	9
	25/ 75	43	49	8
	0/100	34	55	11
HDPE/LLDPE (SC)	100/ 0	81	14	5
	75/ 25	60	25	15
	50/ 50	48	36	16
	25/ 75	40	45	15
	0/100	36	54	10

1) Error \pm 5%.

Diagrams correlating phase distribution and blend composition of the HDPE/VLDPE blends of different thermal histories

(SC and QC) are shown in Fig. 1 and 2. From these phase diagrams, it is very clear that blends containing highly amorphous VLDPE gave a large share of interfacial regions. The fraction of the crystalline phase (P_c) is larger for slowly cooled (SC) specimens than for the corresponding quenched samples, and the fraction of the amorphous phase (P_a) for SC specimens, on the contrary, is smaller. We have found previously that HDPE/VLDPE blends cocrystallize under these conditions (16). Since Raman spectroscopy concerns with molecular vibrations, the preliminary data presented here directed us to rationalize the preferred formation of interfacial regions in a blend of intermolecularly assorted mixtures of short and long crystallites.

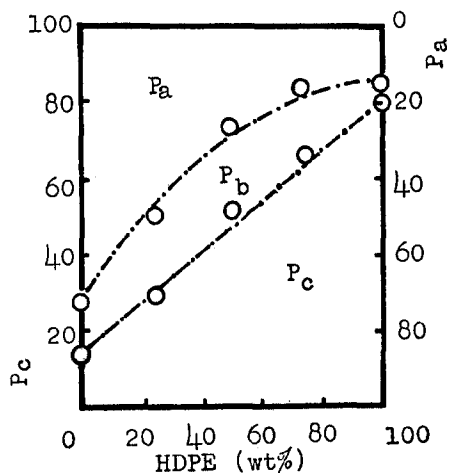


Fig. 1 Phase diagram of HDPE/VLDPE blends (SC)

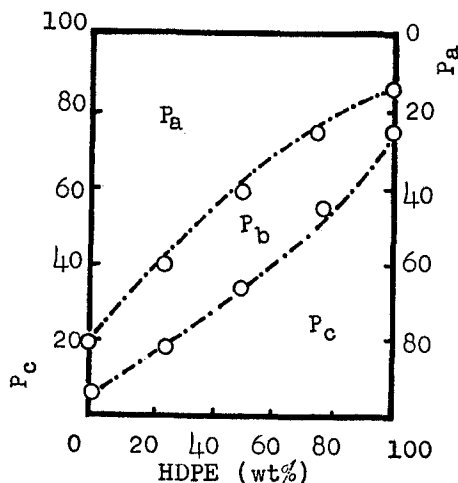


Fig. 2 Phase diagram of HDPE/VLDPE blends (QC)

To further correlate cocrystallizability in blends of polyethylenes and their phase composition, we examined the phase diagrams of HDPE/LDPE and HDPE/LLDPE blends in the same manner. For HDPE/LDPE blends, in line with their known non-cocrystallizability (3,17), the phase constitution of P_c and P_a showed linear additivity with composition (Fig. 3). The fraction of the interfacial region is small (6-9%, Table 2). On the contrary, the cocrystallizable HDPE/LLDPE blends (2,18) have a P_b content of 15-16%, larger than that of their parent polymers. These difference in phase diagrams originate from interactions of different PEs in the blends on a molecular level. While HDPE with a small amount of side-chains (Table 1) has long crystallizable ethylene sequences, LLDPE with abounding side-chains (Table 1) has much shorter ethylene sequences available for crystallization. When HDPE and LLDPE cocrystallize on a molecular scale, the chain protruding out from the crystalline lamellae forming the anisotropic disordered region are much more extensive than in either of the parent polyethylenes having more uniform length of PE sequences. For blends of

non-cocrystallizable pair of HDPE and LDPE, additivity in phase constitution is easily understandable.

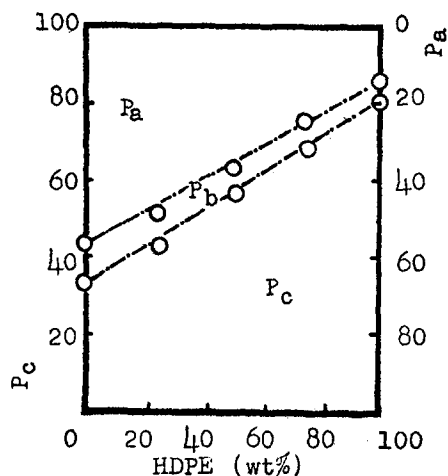


Fig. 3 Phase diagram of HDPE/LDPE blends (SC)

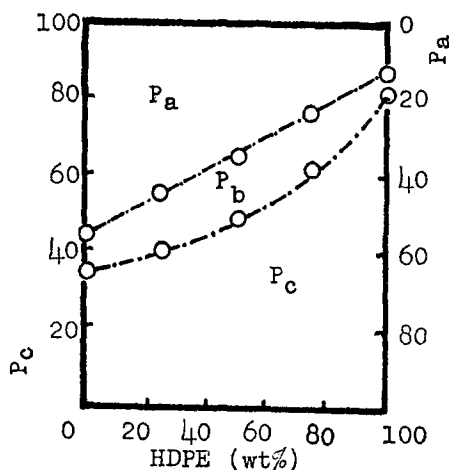


Fig. 4 Phase diagram of HDPE/LLDPE blends (SC)

A good metaphoric vision of variation in the interfacial region of polyethylene blends lies in the case of a bundle of assorted short and long chopsticks. The larger the difference in their length, the longer the region of the non-uniform section above the region of uniform length (Fig. 5).

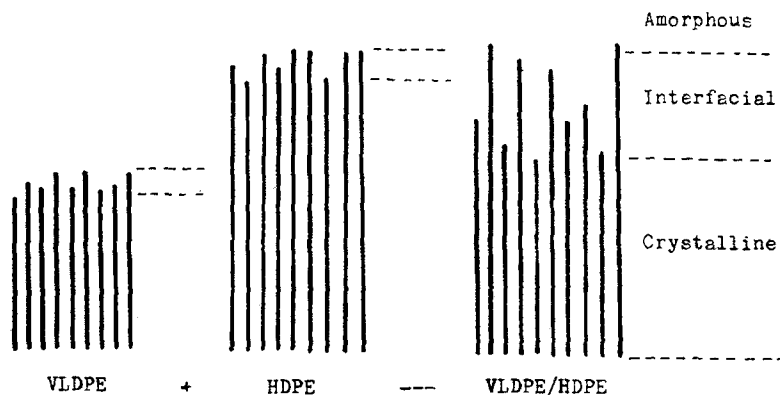


Fig. 5 Schematic representation of transition layer of polyethylene and polyethylene blends

Of methods probing PE blends on a molecular level, IR and NMR, are incapacious due to lack of distinguishable structural features of individual components, though they yield information of PE reentry model through use of blends containing elaborately deuterated PED(19,20). Thus, Raman internal mode region analysis provides an elegant, simple access to direct observing of the compatibility of different PEs on a molecular level. The share of P_b fraction is taken as a sign and measure of cocrystallizability of different polyethylenes.

REFERENCES

1. Donatelli, A. A., J. Appl. Polym. Sci., 23, 3071(1979).
2. Hu, S.-R., Kyu, T., Stein, R. S., J. Polym. Sci., Polym. Phys. Ed., 25, 71(1987).
3. Kyu, T., Hu, S.-R., Stein, R. S., J. Polym. Sci., Polym. Phys. Ed., 25, 89(1987).
4. Ree, M., Kyu, T., Stein, R. S., J. Polym. Sci., Polym. Phys. Ed., 25, 105(1987).
5. Song, H. H., Stein, R. S., Wu, D.-Q., Ree, M., Phillips, J.C., LeGrand, A., Chu, B., Macromolecules, 21, 1180(1988).
6. Kitamaru, R., Horii, F., Hyon, S. H., J. Polym. Sci., Polym. Phys. Ed., 15, 821(1977).
7. Kitamaru, R., Horri, F., Macromolecules, 19, 636(1986).
8. Strobl, G. R., Hagedorn, W., J. Polym. Sci., Polym. Phys. Ed., 16, 1181(1978).
9. Glotin, M., Mandelkern, L., Coll. & Polym. Sci., 260, 182(1982).
10. Flory, P. J., Yoon, D. Y., Dill, K. A., Macromolecules, 17, 862(1984).
11. Yoon, D. Y., Flory, P. J., Macromolecules, 17, 868(1984).
12. Alamo, R., Domszy, R., Mandelkern, L., J. Phys. Chem., 88, 6587(1984).
13. Popli, R., Glotin, M., Mandelkern, L., Benson, R. S., J. Polym. Sci., Polym. Phys. Ed., 22, 407(1984).
14. Wang, J.-G., Pang, D.-R., Huang, B.-T., in Preprints of Symposium on Polymer Syntheses, Polymerization Reactions and Mechanisms, Nanjing, China, November, 1988, p. 263.
15. Alamo, R. G., Glaser, R. H., Mandelkern, L., J. Polym. Sci., Polym. Phys. Ed., 26, 2169(1988).
16. Huang, B.-T., Wang, J.-G., Pang, D.-R., Third European Symposium on Polymer Blends, July 24-26, 1990, Cambridge, paper B3.
17. Clampitt, B. H., J. Polym. Sci., 3, 671(1965).
18. Edward, G. H., Br. Polym. J., 18, 88(1986).
19. Krimm, S., Diss. Faraday Soc., 68, 244(1979).
20. Natarajan, K. M., Samulski, E. T., Cukier, R. J., Nature, 252, 529(1978).